

Enhancing Airfoil Performance through Artificial Neural Networks and Genetic Algorithm Optimization

Mara-Florina NEGOITA^{*,2}, Daniel-Eugeniu CRUNTEANU²,
Mihai-Vladut HOTHAZIE^{*,1,2}, Mihai-Victor PRICOP¹

*Corresponding author

¹INCAS – National Institute for Aerospace Research “Elie Carafoli”,
B-dul Iuliu Maniu 220, 061126, Bucharest, Romania,
hothazie.mihai@incas.ro*, pricop.victor@incas.ro

²“POLITEHNICA” University of Bucharest, Faculty of Aerospace Engineering,
Str. Gheorghe Polizu 1-7, 011061, Bucharest, Romania,
mara.negoita@stud.aero.upb.ro*, daniel.crunteanu@upb.ro

DOI: 10.13111/2066-8201.2023.15.4.17

Received: 23 September 2023/ Accepted: 28 October 2023/ Published: December 2023

Copyright © 2023. Published by INCAS. This is an “open access” article under the CC BY-NC-ND license (<http://creativecommons.org/licenses/by-nc-nd/4.0/>)

Abstract: *As airfoil design plays a crucial role in achieving superior aerodynamic performances, optimization has become an essential part in various engineering applications, including aeronautics and wind energy production. Airfoil optimization using high-fidelity CFD, although highly effective, has proven itself to be time-consuming and computationally expensive. This paper proposes an alternative approach to airfoil performance assessment, through the integration of a deep learning algorithm and a stochastic optimization method. NACA 4-digit parametrization was used for airfoil geometry generation, to ensure feasibility and to reduce the number of input variables. An extensive dataset of airfoil performance parameters has been obtained using an automated CFD solver, laying the foundation for the training of an accurate and robust Artificial Neural Network, capable of accurately predicting aerodynamic coefficients and significantly reducing computational time. Due to the ANN’s predictive capabilities of efficiently navigating vast search spaces, it has been employed as the fitness evaluation method of a multi-objective Genetic Algorithm. Following the optimization process, the resulting airfoils demonstrate significant enhancements in aerodynamic performance and notable improvements in stall behavior. To validate their increased capabilities, a high-fidelity Computational Fluid Dynamics (CFD) validation was conducted. Simulation results demonstrate the approach’s efficacy in finding the optimum airfoil shape for the given conditions and respecting the imposed constraints.*

Key Words: *database, artificial neural network, computational fluid dynamics, hyperbolic mesh, automation, genetic algorithm, optimization*

1. INTRODUCTION

Nowadays, in the field of aeronautics, optimization has become a crucial step in aircraft design, driving advancements in aircraft performance, safety, and sustainability. Within this context, airfoil optimization stands out as a critical part, as it directly influences an aircraft's aerodynamic efficiency, maneuverability, and range. Consequently, optimizing airfoils remains a focal point for engineers and researchers committed to pushing the boundaries of aviation excellence. The airfoil optimization process using high-fidelity CFD typically is

comprised of three main steps: firstly, the airfoil geometry generation using parametrization methods such as NACA 4 digits, Class-Shape Transformation [1] or Bézier Curves [2] representation; secondly, the computational grid generation through structured or unstructured meshing techniques; and finally, the aerodynamic performance determination using high-fidelity CFD solvers. Among these phases, the performance evaluation using CFD solvers is notably the most time consuming [3].

Efforts to reduce this computational cost have been undertaken extensively and recent advancements in artificial neural networks offer promising alternatives for optimization. Specifically, the use of well-trained neural networks provides an opportunity to substitute the traditional performance evaluation step, significantly reducing computational costs, as it has been mentioned in [4]. This substitution holds potential for expediting the optimization process while preserving accuracy, marking a notable advancement in optimization methodologies. However, the neural network's performance depends not only on the size of the database but also on its quality. In this paper, the database generation is performed using high-fidelity CFD performance prediction.

To minimize the computational time required for database generation, an efficient automation process that seamlessly connects airfoil geometry and grid generation has been developed in regard to [5], with the aerodynamic performance prediction designed to NACA 4-digit airfoils. This approach not only ensures the aerodynamic feasibility of airfoils but also significantly reduces the size of the database, ultimately optimizing computational efficiency. Furthermore, the choice of using opensource packages, such as pyHyp [6] for efficient hyperbolic meshing and ADflow [7], as a multiblock structured CFD solver further minimizes the computational time required for database generation. Having a well-trained neural network enables the use of more complex objective functions and constraints that require multiple aerodynamic performance evaluations, thus enabling the use of more feasible optimum airfoils in aircraft design.

2. METHODOLOGY

The methodology that has been used in this article is comprised of geometry and mesh generation automation, coupled with high-fidelity CFD aerodynamic prediction to generate the database required for the neural network training. Then, a stochastic optimization approach based on genetic algorithm is employed where the aerodynamic performance prediction required in the objective function formulation is used to find the optimum airfoil shape. Then a CFD validation is performed to further validate the obtained results.

A. Airfoil Parametrization Technique

To this date, many parametrization methods have been developed such as Class-Shape Transformation, Hick-Henne, Parsec, Bezier or Spline based curve representations but none of them can impose geometric constraints useful in designing feasible airfoils such as maximum thickness or camber value or position except for the NACA parametrization methods. Thus, NACA 4 digits parametrization method has been chosen for airfoil shape generation defined by three parameters: (M) the designated maximum camber, (P) the position of the maximum camber and (T) the maximum thickness.

B. Mesh Generation

After the geometry is obtained, hyperbolic grid generation is employed for a smooth, orthogonal and high-quality mesh. Moreover, hyperbolic extrusion law ensures smooth and

finer mesh near the wall while preserving local good grid quality criteria for all cells. This meshing technique is used with the help of the open-source package pyHyp, swiftly generating multiblock grids based on a given surface grid, which in this case are the points that define the airfoil's geometry. In the figure below, a grid representation is shown for a NACA0012 airfoil where the mesh near the leading and trailing edge is highlighted.

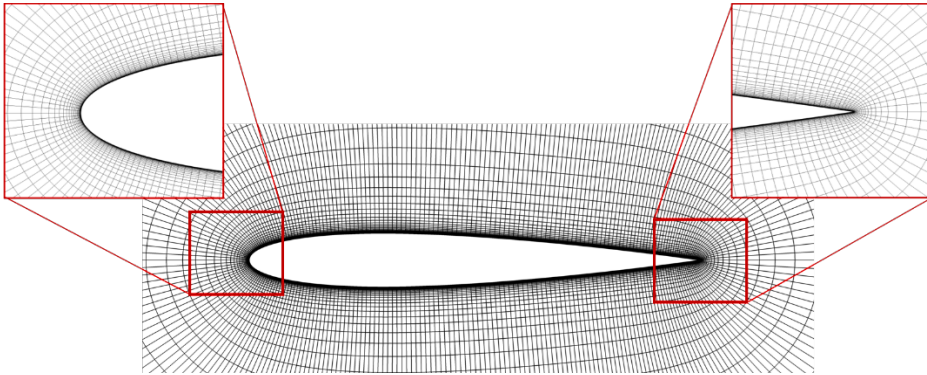


Figure 1. Mesh generation representation highlighting the leading and trailing edge surface point clustering

The use of pyHyp enables the export of structured multiblock grids in CGNS format used by ADflow solver, a high-fidelity CFD solver that was designed to be used in conjunction with this meshing tool, thus making it the most suitable choice for an efficient and easy coupling in the automation process that was needed in our work. It is based on the compressible Reynolds-averaged Navier-Stokes (RANS) equations with a turbulence modelling based on the Spalart-Allmaras equations. The efficient use of Newton-Krylov algorithm for aerodynamic performance prediction minimized the computational time required for individual evaluation, thus further improving the overall computational efficiency of the automation loop.

Having the automation loop developed, a database is constructed using NACA 4 digits airfoils at a Reynolds number of 6 million. The parameters were varied as follows: the maximum camber (M) from 0 to 6, the position of the maximum camber from 1 to 6 and the maximum thickness from 9 to 16, all with an increment of 1, making the total data base consisting in 336 airfoils. Every airfoil was evaluated at 17 angles of attack ranging from -8 to 15 degrees.

C. Artificial Neural Networks

Neural networks represent nature-inspired computational models, capable of learning complex patterns and accurately reproducing non-linear data behavior. Due to their extensive capabilities of modeling input-output data consisting of several independent parameters, ANNs are suitable for predicting aerodynamic coefficients of different airfoils, without any previous knowledge of the underlying physical processes [8].

A deep neural network has been implemented using the Deep Learning Toolbox in MATLAB. The training dataset provided to the ANN is based on the generated data base based on CFD predictions. For each airfoils available for analysis, the coefficients of the NACA 4 digits parametrization method were used as input data as well as the lift and drag coefficient at the specified range of angles of attack. To assess the model's generalization performance, the dataset was split into a training data set, consisting of 80% of the initial data, and a testing one, containing the remainder 20% of the data.

The preferred deep neural network consists of an input layer and 4 hidden layers, enabling the model to learn complex patterns and relationship between the data, and an output layer,

providing the prediction. A visual representation of the network’s architecture is presented in the figure below.

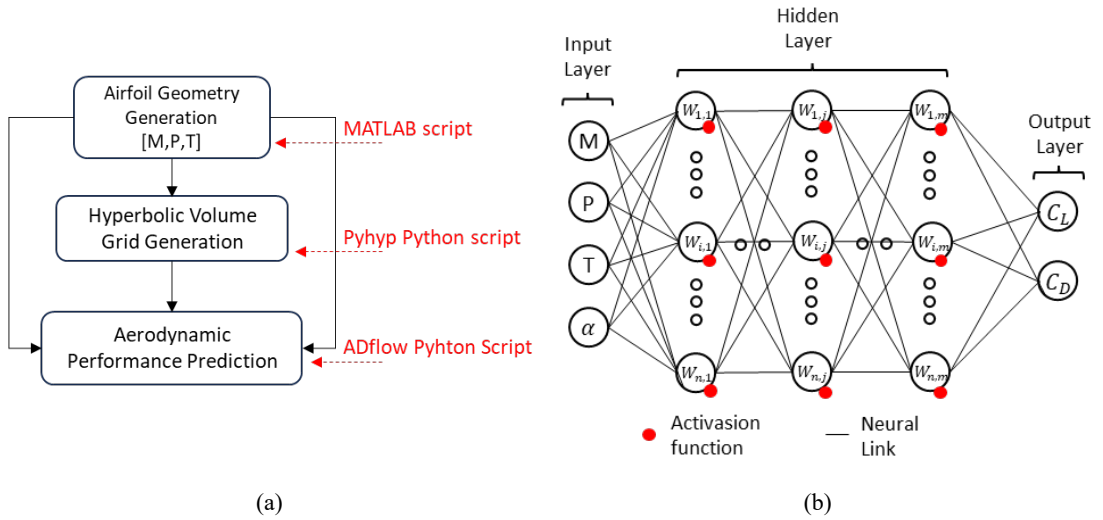


Figure 2. Automation loop (a) and architecture of the neural network (b)

The input layer consists of six ($M, P, T, \alpha, C_L, C_D$) artificial neurons, one for every training variable. After being passed through the input layer, to each neuron is assigned a weight value and a bias by the first hidden layer. Each hidden layer disposes of an activation function, introducing non-linearity into the model and enabling it to approximate complex functions [8]. During the backpropagation process, the network iteratively repeats the forward and backward passes on training data, adjusting weights and biases to improve prediction accuracy.

$$y = f\left(\sum_{i=1}^n w_i \cdot x_i + b_i\right) = f(W^T \cdot X + B) \tag{1}$$

where W^T denotes the matrix of weights. X is the vector of inputs, B is the bias and f the activation function. ReLU (Rectified Linear Unit) was used as the activation function in both the hidden and the output layer, due to its effectiveness in regression models and computational capability [8].

The model’s accuracy was evaluated by the loss function, Mean Square Error (MSE), quantifying the difference between the predicted and the initial values. Adaptive Moment Estimation (ADAM) was used as the optimization function, as it enables individual learning for each of the parameters. The network was trained for 20000 epochs in multiple batches of data, each consisting of 100 samples.

D. Genetic Algorithm

Genetic algorithms represent stochastic optimization techniques inspired by the process of natural selection. Although many optimization methods are in use [9], [10], this type of evolutionary algorithms prove themselves particularly efficient in solving complex problems, with multiple optimization variables and large design space exploration requirements. Airfoil optimization is often achieved through GA, due to the method’s stochastic character and increased performance in complex problems [11], [12]. In order to obtain the most suitable

airfoil shape for the given conditions, a multi-objective, constrained optimization program has been implemented in MATLAB, using genetic algorithms.

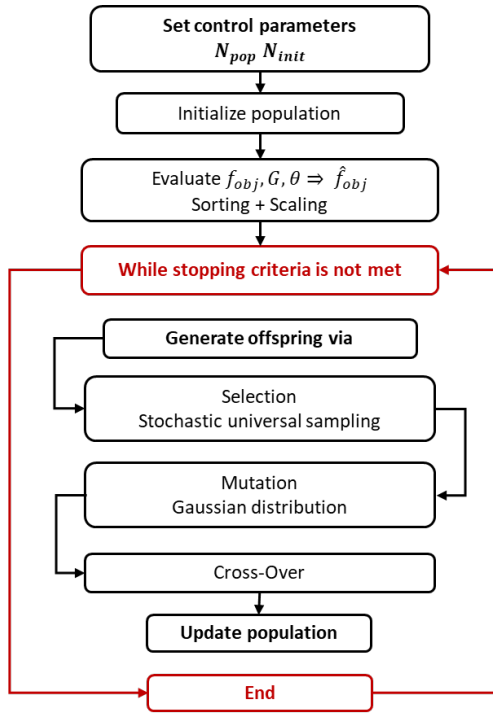


Figure 3. Genetic Algorithm optimization flow chart

The chosen optimization variables represent the three parameters dictating the airfoil geometry M , P and T . The fitness functions are evaluated by using the already trained neural network, predicting aerodynamic coefficients at different angles of attack. Therefore, the three objective functions the algorithm must preserve are: minimizing C_D as well as $dC_D/d\alpha$ at 2° , maximizing the lift-to-drag coefficient C_L/C_D at an angle of attack of 15° .

During each generation, a random initial population is selected for evaluation, and, based on their performance, only the individuals with the lowest fitness value survive to the next generation. This step represents the selection, providing a stochastic mechanism that introduces diversity and allows an efficient exploration of the search space. Stochastic Universal sampling was used in as the selection type in this optimization, due to the method’s accuracy and computational advantages over other models [12]. A subset of individuals was chosen to undergo a Gaussian mutation, to ensure diversity and avoid premature convergence. Due to the low number of decision variables, a mutation rate of 0.15 was chosen, to prevent the algorithm from converging into local minima.

For ensuring faster convergence of the algorithm and a well-defined set of optimal solutions on the Pareto front, constraints and boundaries have been implemented.

Table 1. Boundary conditions

+Boundary Type	M	P	T
Lower	1	1	9
Upper	5	6	14

As the optimization is performed with respect to multiple objective functions, no single optimum solution is possible. Therefore, several best individuals are selected, their

performance being subject to a trade-off between the two objective functions and the respected constraints. The imposed constraints allow only the most-feasible, best-performing individuals to define the Pareto front.

Objective	$minimize C_D(\alpha), \alpha = 2^\circ$
	$minimize C_D/C_L(\alpha), \alpha = 15^\circ$
	$minimize \left(\frac{dC_D}{d\alpha}\right)_{\alpha=2}$
Constraint	$Area_{optimum\ airfoil} \geq Area_{NACA0012}$

3. RESULTS

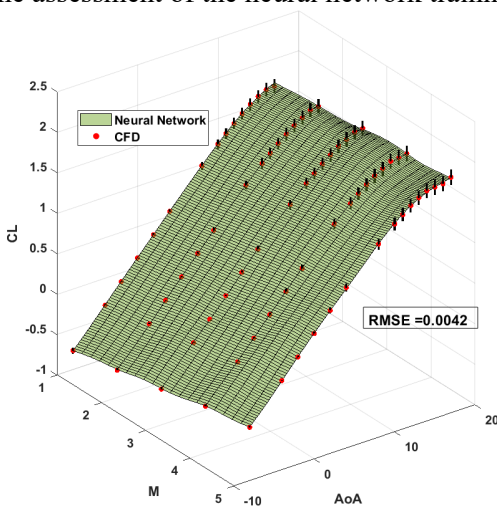
The following chapter presents the numerical results and interpretation of the airfoil optimization process through the integration of Artificial Neural Networks (ANNs) and Genetic Algorithm (GA).

Results are divided into two parts: the initial part presents the accuracy level of the trained neural network, while the latter shows the optimization process, emphasizing the optimization convergence and results interpretation.

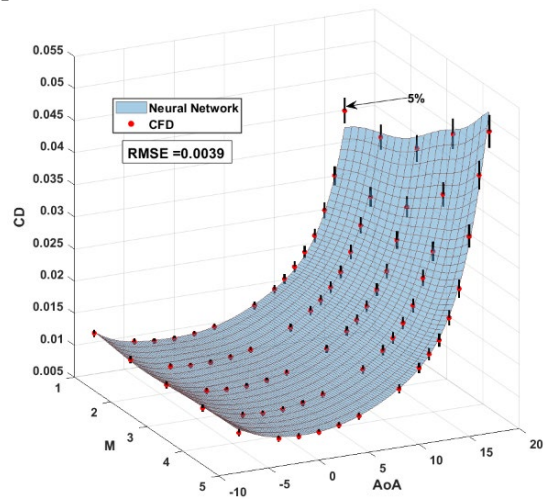
A. Neural Network Results

For the aerodynamic prediction of both lift and drag coefficients, two independent deep neural networks have been implemented and trained on the CFD generated database. Figure 4 (a)-(f) provides a comparative analysis between the initial and the predicted values, for a wide range of angles of attack, alongside the variation of the input parameters M (Figure 4 (a) and 4(b)), P (Figure 4(c) and (d)) and T (Figure 4 (e) and (f)).

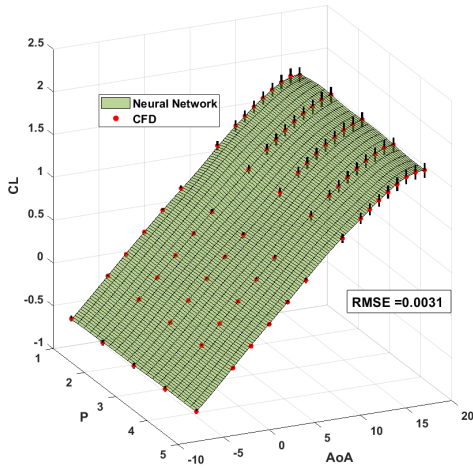
The proposed NACA 4-digit parametrization method allows for the data to be visualized in representative planes, which, in turn, enhances data interpretation. This approach facilitates the assessment of essential aerodynamic airfoil properties, including parameters like maximum curvature (M), thickness (T), and the location of maximum camber (P), as well as the assessment of the neural network training performance.



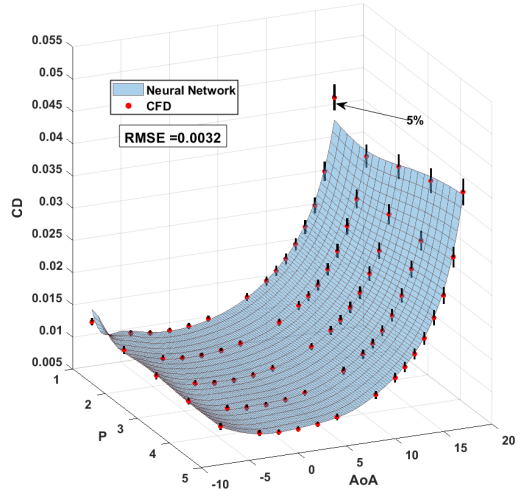
(a) C_L vs AoA vs M , for $P = 4$ and $T = 12$



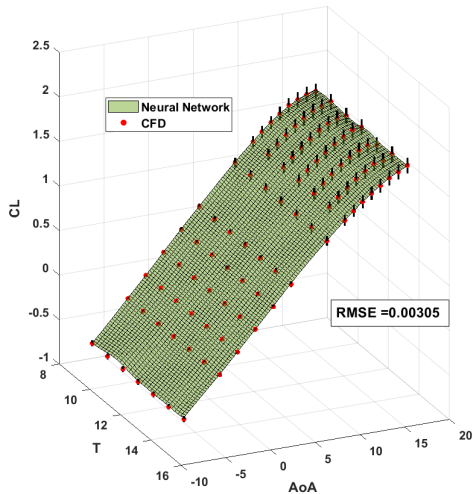
(b) C_D vs AoA vs M , for $P = 4$ and $T = 12$



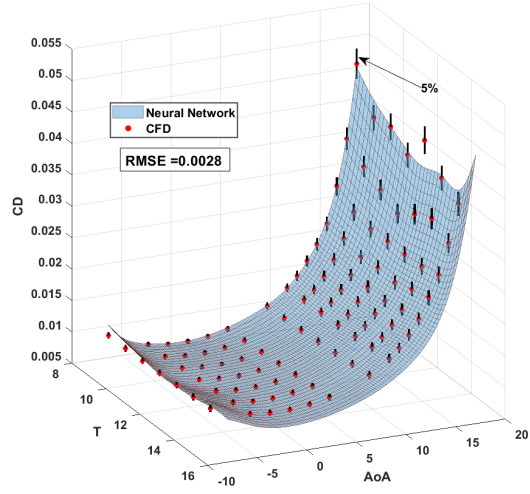
(c) C_L vs AoA vs P , for $M = 2$ and $T = 12$



(d) C_D vs AoA vs P , for $M = 2$ and $T = 12$



(e) C_L vs AoA vs T , for $M = 2$ and $P = 4$



(f) C_D vs AoA vs T , for $M = 2$ and $P = 4$

Figure 4. Comparative parametric analysis between CFD and Neural Network predicted data

The reduced order of the root mean square error for both lift and drag representations prove the efficiency of the chosen method as a way of generating aerodynamic coefficients, as the trained Neural Network exhibits feasible results for the chosen angles of attack.

Certain inconsistencies exist for higher AoA values, notably regarding the drag coefficient, due to the non-linear behavior of the provided training data. Nevertheless, the 5% error bar is only surpassed for AoA values higher than 16° , demonstrating the performance of the trained model.

The accuracy of the NN model is evaluated not only throughout the comparison between the initial and the predicted values, but also through the training process.

This assessment is shown in Figure 5, (a) displays the histogram representing the gradient loss function over the course of training epochs.

As the gradient guides the weight updates during the training process, the performance on the neural network increases.

A decrease in the descent rate below 10^{-6} indicates an improved convergence of the algorithm and reduced weight adjustments, signaling an increased efficiency of the regression model.

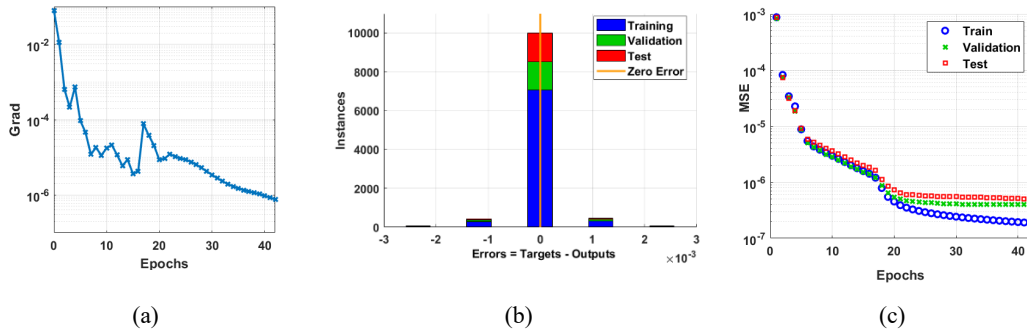


Figure 5. Gradient vs Epochs (a), Error Histogram (b) and MSE vs Epochs (c).

Figure 5 (b) and (c) present the error distribution during the training process. The narrow-centered, Gaussian-like distribution of the Error Histogram indicates reduced error values and efficient learning.

Alternatively, the Mean Square Error (MSE) is plotted with respect to the number of epochs, proving the convergence to optimality of the Training, Validation and Testing data alike. The MSE decrease rate stabilizes after 30 epochs, indicating optimal weights and an efficient training process.

As the trained deep neural network consistently demonstrates enhanced performance throughout training, validation, and testing, with reduced errors across extensive datasets covering a wide range of angles of attack, it has been deemed sufficiently robust to serve as the fitness evaluation function for the optimization algorithm.

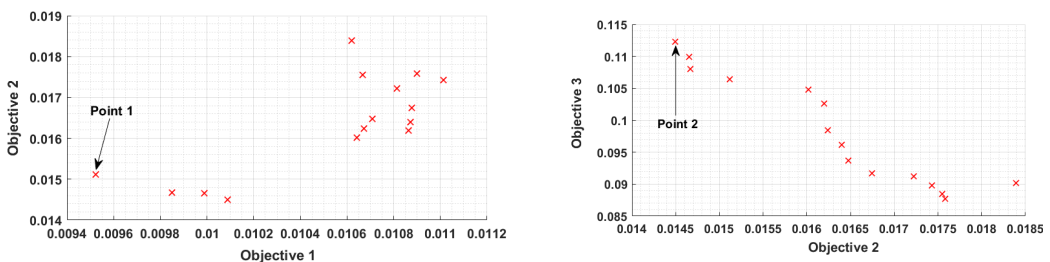
B. Genetic Algorithm Multi-Optimization Results

The multi-objective optimization algorithm reached convergence at around 100 generations with a population size of 50 and a minimum variation of the Pareto front less than 10^{-4} .

Figure 6 displays the Pareto front representing a series of optimum individuals with different values for their respective objective functions.

In addition, the smooth behavior of the Pareto front combined with the relatively limited range of variation in the objective function across all points within the Pareto set, demonstrates efficient space exploration.

The optimization algorithm performed 100 generations before reaching the Pareto front shown in Figure 7, displaying a series of optimum solutions. The smooth curve formed by the displayed points indicates an efficient space exploration, ensuring viable results.



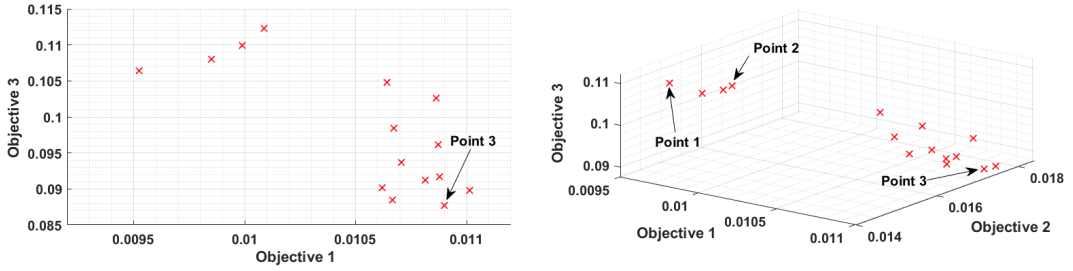


Figure 6. Pareto Front Representation

As a multi-objective GA displays multiple optimum solutions, each of them representing a trade-off between the objective performances, more than one result must be considered when inspecting efficiency. Table 3 presents three individual solutions, representing the points situated closest to each axis. As expected, the extreme solutions exhibit minimum values for one of the objective functions, but also perform well in the others. Therefore, every point on the Pareto front represents a suitable, viable solution to the presented optimization.

Table 3. Comparison between distinct points in the Pareto front

Point on the Pareto front	M	P	T	Objective 1 ($C_D(2)$) · 10 ⁻⁴	Objective 2 ($C_D/C_L(15)$)	Objective 3 ($\frac{dC_D}{d\alpha}$) _{α=2}
Point 1	1.85	3.07	11.94	95	0.0151	0.1064
Point 2	2.35	3.13	13.12	101	0.0144	0.1123
Point 3	4.57	3.35	12.17	108	0.0175	0.0877

The visual representation in Figure 7 of the optimized airfoils demonstrates the influence of geometric parameters in airfoil performance. Although the location of the maximum camber remains consistent among the three positions, there is a significant difference in the magnitude of the maximum camber between them. Point 1 exhibits the lowest maximum camber, denoted as M, as well as the lowest maximum thickness, resulting in the least amount of drag among the three positions as shown in Figure 7. However, when examining the lift-to-drag ratio curve, the superior drag performance translates into a comparatively inferior lift-to-drag ratio when compared to the last individual.

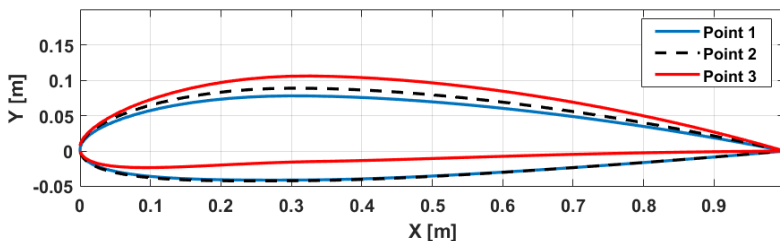


Figure 7. Comparison between the geometry of the selected individuals from the Pareto front

Point 3, which boasts the highest maximum camber and maximum thickness among the three, excels in terms of lift coefficient. Nevertheless, it comes with a notable drawback in the form of the drag coefficient, particularly at angles of attack ranging from 4 to 16 degrees. When comparing all three points, we observe similar behaviors between Points 1 and 2, but Point 3 stands out with significant different performance highlighted in the favorable stall characteristics. All results have been obtained using the same Neural Network employed in the optimization method. Furthermore, a CFD validation has been performed on the airfoil

represented as Point 1, proving not only the efficiency of the Genetic Algorithm optimization, but also the high accuracy of the trained Neural Network.

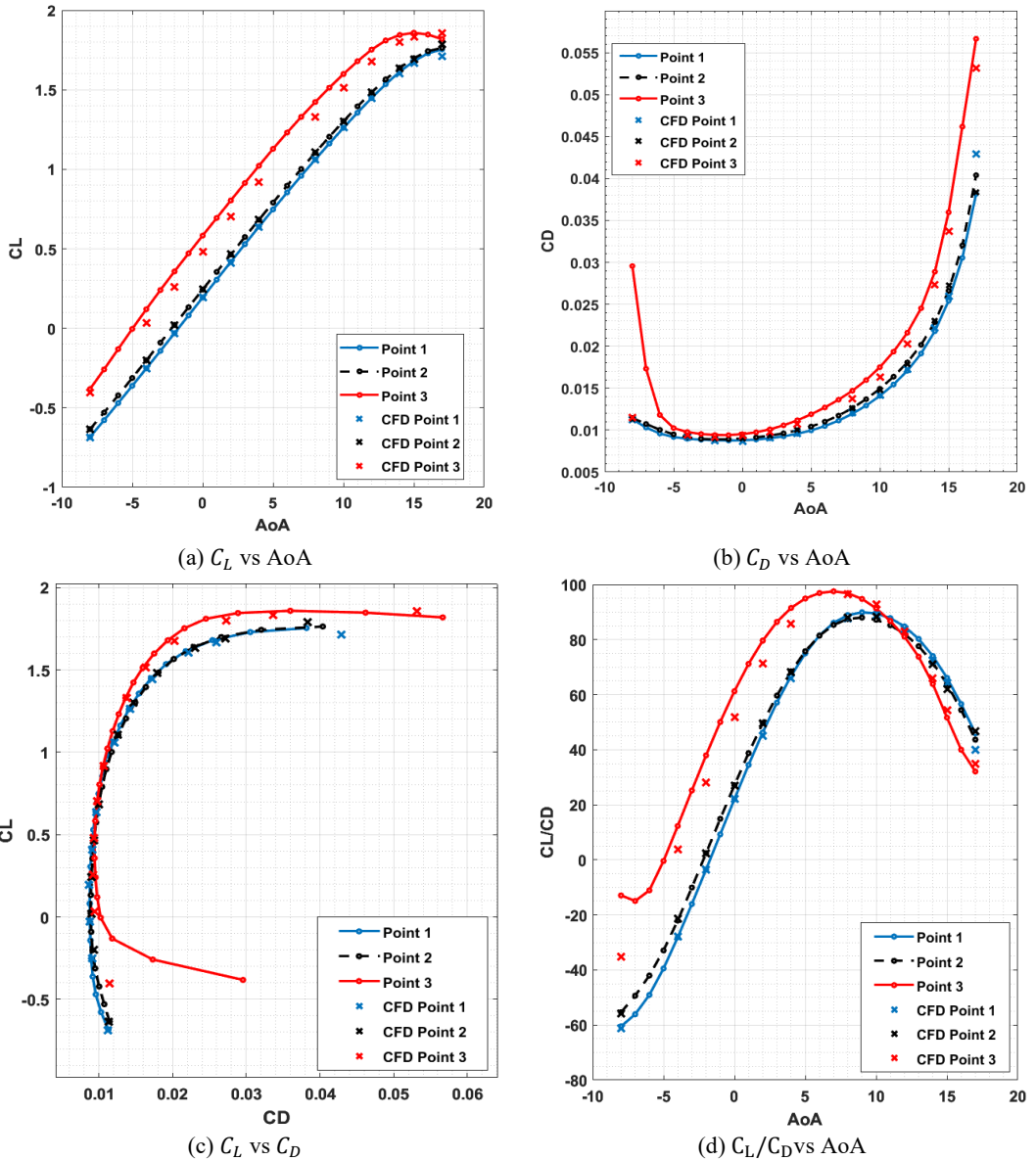


Figure 8. Comparative performance of the optimized airfoils

4. CONCLUSIONS

The aim of this paper was to propose an alternative approach to airfoil optimization, based on the integration of a deep-learning neural network algorithm coupled with a multi-objective stochastic optimization algorithm. The Artificial Neural Network was trained on a comprehensive dataset of NACA 4-digit airfoil performances, obtained using an automated CFD procedure. The chosen parametrization method and automation process have proven to be a convenient coupling, generating an extensive training database.

The employed ANN impressive performance represents an effective, yet robust and computationally efficient regression model. Nonetheless, the Neural Network's performance is crucially influenced by its architecture, any variation in the network's hyper parameters leading to changes in the model's prediction capabilities. As the trained ANN represents a reliable and time efficient prediction method, its integration in a multi-objective Genetic Algorithm optimization has enabled us a significant computational effort reduction. Furthermore, the efficiency of this approach allows us to use multiple objective functions with minimal computational time added, enabling us to define and employ complex optimization processes with more relevant objective functions and constraints.

Consequential to the type of objective functions of the optimization method, a series of suitable solutions have been found. All these cases represent relevant solutions and should be taken into account, allowing for the selection of the most suitable individual based on the specific requirements from the Pareto front.

To conclude with, the integration of a deep learning neural network model in a constrained multi-objective Genetic Algorithm airfoil optimization has resulted in valid, highly performant solutions. This approach's success lays the foundation for further exploration and future work, exploring with different parametrization methods, various objective functions, and constraints.

ACKNOWLEDGEMENT

The paper “*Enhancing Airfoil Performance through Artificial Neural Networks and Genetic Algorithm Optimization*” has been awarded with the “Caius Iacob” Prize during the **40th edition of the Conference “Caius Iacob” on Fluid Mechanics and its Technical Applications**, in 19 - 20 October 2023, organized by the INCAS – National Institute for Aerospace Research “Elie Carafoli”.

REFERENCES

- [1] B. M. Kulfan, Universal parametric geometry representation method, *Journal of Aircraft*, vol. **45**, no. 1, pp. 142-158, 2008.
- [2] T. Melin, Parametric Airfoil Catalog, *An Aerodynamic and Geometric Comparison Between Parametrized and Point Cloud Airfoils*, Linköping, Sweden: Fluid and Mechatronic Systems, 2013.
- [3] D. Dimitris, Computational aerodynamics: Advances and challenges, *The Aeronautical Journal*, vol. **120**, no. 1223, pp. 13-36, 01/2016.
- [4] K. H. Z. I. Moin Hassan, Airfoil's Aerodynamic Coefficients Prediction using Artificial Neural Network, in *19th International Bhurban Conference on Applied Sciences and Technology (IBCAST)*, 2022.
- [5] G. F. F. H. F. B. C. M. M and B. C. A highly automated method for simulating airfoil characteristics at low Reynolds number using a RANS - transition approach, in *Deutscher Luft- und Raumfahrtkongress 2019*, Darmstadt, 2019.
- [6] * * * “pyhyp,” [Online]. Available: <https://github.com/mdolab/pyhyp>.
- [7] * * * “ADflow,” [Online]. Available: <https://mdolab-adflow.readthedocs-hosted.com/en/latest/citation.html>.
- [8] B. S. d. M. R. d. M. G. Mailema Celestino dos Santos, Aerodynamic Coefficient Prediction of Aircraft Using Neural Network, in *19th International Congress of Mechanical Engineering*, Brasília, 2007.
- [9] K. Slawomir and L. Leifur, Multi-level CFD-based Airfoil Shape Optimization with, *2013 International Conference on Computational Science*, p. 11, 2013.
- [10] S. W. J. Dussauge Thomas P., A reinforcement learning approach to airfoil shape optimization, *Nature Publishing Group*, vol. **13**, no. 1, 2023-06-16
- [11] Z. Jinhuan, An improved genetic algorithm and its applications to the optimisation design of an aspirated compressor profile, *International Journal for Numerical Methods in Fluids*, vol. **79**, no. 12, pp. 640-653, 2015.
- [12] L. Xiao, Rapid design and optimization of airfoil based on improved genetic algorithm, *Publisher: Acta Aerodynamica Sinica*, Dec 25, 2016.